City Research Online

City, University of London Institutional Repository

Complex BPS Skyrmions with real energy

Francisco Correa [b], Andreas Fring [a,*], Takanobu Taira [a]

[a] *Department of Mathematics, City, University of London, Northampton Square, London EC1V 0HB, UK*
[b] *Instituto de Ciencias Físicas y Matemáticas, Universidad Austral de Chile, Casilla 567, Valdivia, Chile*

Abstract

We propose and investigate several complex versions of extensions and restrictions of the Skyrme model with a well-defined Bogomolny-Prasad-Sommerfield (BPS) limit. The models studied possess complex kink, anti-kink, semi-kink, massless and purely imaginary compacton BPS solutions that all have real energies. The reality of the energies for a particular solution is guaranteed when a modified antilinear $\mathcal{CPT}$-symmetry maps the Hamiltonian functional to its parity time-reversed complex conjugate and the solution field to itself or a new field with degenerate energy. In addition to the known BPS Skyrmion configurations we find new types that we refer to as step, cusp, shell, and purely imaginary compacton solutions.

1. Introduction

The Skyrme model [1] has been introduced as a potential candidate for a low energy effective field theoretical description of a strongly interacting matter theory, i.e. Quantum Chromodynamics, more than fifty years ago. It took a fairly long time to demonstrate that the model could indeed arise as such type of low energy effective theory in a limit for which the number of quark colours is taken to be very large [2,3]. The Skyrme model is perfectly tailored to the nonperturbative nature of that energy regime and successfully describes various key characteristics of atomic nuclei. The topological soliton solutions of the model, the Skyrmions, are identified as

Baryons with integer topological charges B being elements in the third homotopy group for the $SU(2)$-group valued fields, $B \in \mathbb{Z} \simeq \pi_3(SU(2))$. The field excitations around a trivial vacuum are identified as pions [4–6] and there exist also variants of the model that include ρ, ω and A_1 vector mesons [7,8]. Early on in the exploration of the model it was also noticed that Skyrmions allow for a fermionic interpretation [9] and that one may formulate gauge theoretical versions of them [10]. Atiyah and Manton established the remarkable fact that static Skyrmion solutions in $\mathbb{R}^3$ can be approximated well by holonomies of $SU(2)$ Yang-Mills instantons in $\mathbb{R}^4$ [11,12].

Despite the success of the model on qualitative and conceptual aspects, it is still way off on a quantitative level when comparing numerical solutions to experimental measurements [13], as most quantities differ by a fair amount, such as for instance the magnetic moments for the protons and neutrons which are too small by about 30%. The Euler-Lagrange equation associated to the Skyrme model is a complicated nonlinear wave equation for which various solutions have been obtained numerically for small and large Baryon numbers [14–16,5,17–19]. The energies for all these solutions show that the binding energy, that is the energy required to separate a multi-Skyrmion solution into single Skyrmions normalized by the Baryon number, is far too large when compared to what is expected from experiments. Motivated by trying to address this discrepancy, different variants of the original Skyrme model have been explored. Especially promising are versions of the model with a well-defined Bogomolny-Prasad-Sommerfield (BPS) [20,21] limit as originally proposed in [22].

These models exhibit a number of very appealing features: Firstly, they allow for the construction of elegant exact analytical solutions in form of topological solitons that satisfy the Bogomolny bounds. Secondly they reproduce the linear relation between the binding energies and the baryon number for small and large values. Thirdly, and most importantly, they resolve the issue of the discrepancy of the large binding energies in the original Skyrme model. In fact, in the BPS versions of the model the binding energies are zero and one may adopt the view that quantum corrections will only introduce small variations, hence producing the expected smaller values for the binding energies. Taking corrections from collective coordinate quantization of spin and isospin, the electrostatic Coulomb energies, and small explicit breaking of the isospin symmetry into account lead to a very good agreement between theory and experimental values for the binding energy as shown in [23–25]. For a recent review on these type of BPS Skyrme models see [26].

Motivated by the success of the BPS versions of the original Skyrme model, we explore here further possible variants that include complex non-Hermitian versions of these models. We demonstrate that some of their static solutions have real topological energies despite being complex and thus these solutions may also be associated to well-defined physical objects.

In order to overcome the so-called auxiliary field problem and emergence of fourth-order time derivatives when introducing supersymmetry, complex versions of the Skyrme model were previously studied [37,38], by taking the fields to be valued in a complexification of $SU(N)$, i.e. $SL(N, \mathbb{C})$. Besides trying to overcome the above mentioned problems, these studies were guided by the fact that the introduction of supersymmetry into the Skyrme model is almost inevitably forcing the introduction of complex structures as the underlying manifolds need to be of Kähler type for this purpose. However, complex solutions and their reality conditions were not considered previously.

As argued in [27] the reality of the energy for some scalar field solutions ϕ_i, $i = 1, 2, \ldots$, to the BPS equations or the equations of motion is guaranteed when the following three conditions are met:

(i) There exists a modified $\mathcal{CPT}$-symmetry that maps the Hamiltonian functional to its parity time-reversed complex conjugate

$$\mathcal{CPT} : \mathcal{H}[\phi(x_\mu)] \to \mathcal{H}^\dagger[\phi(-x_\mu)], \tag{1.1}$$

with $\mathcal{CPT}^2 = \mathbb{I}$. Here $\mathcal{CPT}$-symmetry is not to be taken literally as a simultaneous parity, time reversal and charge conjugation, but be understood simply as an antilinear map of any kind in the sense described by Wigner in [28].

(ii) Two solutions ϕ_i and ϕ_j, not necessarily distinct, are related to each other by the modified $\mathcal{CPT}$-symmetry as

$$\mathcal{CPT} : \phi_i(x_\mu) \to \phi_j(-x_\mu). \tag{1.2}$$

(iii) The energies $E[\phi]$ of the two solutions ϕ_i and ϕ_j are degenerate

$$E[\phi_i] = E[\phi_j]. \tag{1.3}$$

Evidently when $\phi_i = \phi_j$ this condition holds trivially and the energy is automatically guaranteed to be real. When $\phi_i \neq \phi_j$ we must ensure that the energies are degenerate to reach the same conclusion. As we shall see below this is often a consequence of some symmetries in some coupling or integration constants or by the fact that energies for solutions of the self-dual and anti-self-dual BPS equations are identical as argued in [27].

For a more detailed reasoning on why these conditions and further examples we refer the reader to [27] and references therein. We will present examples below for models with solutions satisfying all three conditions so that their energies are real, but we shall also explore the broken $\mathcal{CPT}$-regime by presenting counter examples for solutions with complex energies for which either or both conditions (ii) and (iii) do not hold.

Our manuscript is organized as follows: In section 2 we recall a general Lagrangian density that encompasses a whole set of extensions and restrictions of the standard version of the Skyrme model. In sections 3 we discuss a complex, albeit pseudo Hermitian, version of the Skyrme model that possess new types of solutions that satisfy all three conditions (1.1)-(1.3) and have therefore real energies. In section 4 we discuss a version of the BPS Skyrme model with a potential that leads to solutions that behave asymptotically as kinks but with finite values a zero and also massless solutions with zero energy. In section 5 we discuss a version of the model involving a whole ray of Bender-Boettcher type potentials that possess fractional compacton and semi-kink solutions with real energies. In section 6 we explore the broken $\mathcal{CPT}$-regime by discussing a model for which either condition (ii) and/or condition (iii) are not satisfied. Section 7 contains a discussion of a Skyrmion submodel with complex semi-kink and soliton-like solutions. Our conclusions are stated in section 8.

2. The Skyrme model - extensions and restrictions

To establish our notations and conventions we briefly recall some key aspects and definitions of the Skyrme model. Largely following [22,26], we consider an extended version of the standard Skyrme model described by variants of a Lagrangian density of the general form

$$\mathcal{L} = \tilde{\mathcal{L}}_0 + \mathcal{L}_2 + \mathcal{L}_4 + \mathcal{L}_6 + \mathcal{L}_0, \tag{2.1}$$

where the different terms are defined as

$$\mathcal{L}_2 := -\frac{f_\pi^2}{2}\operatorname{Tr}\left(L_\mu L^\mu\right), \quad \mathcal{L}_4 := \frac{1}{16e^2}\operatorname{Tr}\left([L_\mu, L_\nu]^2\right),$$

$$\mathcal{L}_6 := -\lambda^2 N_0^2 B_\mu B^\mu, \quad \mathcal{L}_0 := -\mu^2 V, \tag{2.2}$$

with Lie algebraic currents in form of right Maurer Cartan forms, topological current and $SU(2)$-group valued Skyrme fields

$$L_\mu := U^\dagger \partial_\mu U, \quad B^\mu := \frac{1}{N_0}\varepsilon^{\mu\nu\rho\tau}\operatorname{Tr}\left(L_\nu L_\rho L_\tau\right), \quad U := e^{i\zeta(\sigma\cdot\vec{n})}, \tag{2.3}$$

respectively. Here f_π can be interpreted as the pion decay constant and the dimensionless constant e is referred to as the Skyrme parameter. As is well known, these parameters can be scaled away, so that we may set them both to 1 in what follows. Moreover, we denote by σ the standard Pauli matrices and take the three component unit vector to be of the form $\vec{n} = (\sin\Theta\cos\Phi, \sin\Theta\sin\Phi, \cos\Theta)$ rather than the rational map or stereographic projection often used instead in this context, see e.g. [29]. Our space-time metric g is taken to be diag $g = (1, -1, -1, -1)$. The normalization constant N_0 is chosen in such a way that the Baryon number $B = \int B_0 d^3x \in \mathbb{Z}$ becomes an integer as it should be for a two flavour theory to guarantee that Baryons with an even and odd number of quarks are Bosons and Fermions, respectively. See for instance [3] for a more detailed reasoning on this issue. For a standard static compacton solution the normalization constant is usually taken to be $N_0 = 24\pi^2$.

Dropping and decomposing terms or further specifying the potential in the general Lagrangian $\mathcal{L}$ gives rise to different versions of the model. The original Skyrme model [1] is comprised of the sum of the sigma model term $\mathcal{L}_2$ and the Skyrme term $\mathcal{L}_4$ with occasionally the potential term $\tilde{\mathcal{L}}_0$ added which is of the same functional form as $\mathcal{L}_0$. The BPS version of the model introduced in [22] consists of the sum of $\mathcal{L}_6$, that mimics the interactions generated by the vector mesons, and the potential term $\mathcal{L}_0$.

Consistent submodels may be obtained by further decomposing terms in $\mathcal{L}$. With our choice of the parameterization for the $SU(2)$-group valued element U the various parts of the Lagrangian take on the following forms: For reasons that will become clear below, we decompose the sigma model and the Skyrme term as

$$\mathcal{L}_2 = \mathcal{L}_2^{(1)} + \mathcal{L}_2^{(2)}, \quad \text{and} \quad \mathcal{L}_4 = \mathcal{L}_4^{(1)} + \mathcal{L}_4^{(2)}, \tag{2.4}$$

with

$$\mathcal{L}_2^{(1)} = \sin^2\zeta\left(\Theta_\mu\Theta^\mu + \Phi_\mu\Phi^\mu\sin^2\Theta\right), \tag{2.5}$$

$$\mathcal{L}_2^{(2)} = \zeta_\mu\zeta^\mu, \tag{2.6}$$

$$\mathcal{L}_4^{(1)} = \sin^2\zeta\left[\Theta_\mu\zeta^\mu\Theta_\nu\zeta^\nu - \Theta_\mu\Theta^\mu\zeta_\nu\zeta^\nu + \sin^2\Theta\left(\Phi_\mu\zeta^\mu\Phi_\nu\zeta^\nu - \Phi_\mu\Phi^\mu\zeta_\nu\zeta^\nu\right)\right], \tag{2.7}$$

$$\mathcal{L}_4^{(2)} = \sin^4\zeta\sin^2\Theta\left(\Theta_\mu\Phi^\mu\Theta_\nu\Phi^\nu - \Theta_\mu\Theta^\mu\Phi_\nu\Phi^\nu\right). \tag{2.8}$$

The extended part computes with

$$B^\mu = \frac{1}{2N_0}\sin^2\zeta\sin\Theta\,\mathcal{B}^\mu, \quad \mathcal{B}^\mu := \varepsilon^{\mu\nu\rho\tau}\zeta_\nu\Theta_\rho\Phi_\tau \tag{2.9}$$

to

$$\mathcal{L}_6 = -\frac{\lambda^2}{4}\sin^4\zeta\sin^2\Theta\mathcal{B}_\mu\mathcal{B}^\mu = \frac{\lambda^2}{4}\sin^4\zeta\sin^2\Theta\left[\varphi_0^a\mathcal{Q}_a^i\varphi_0^b\mathcal{Q}_b^i - \mathcal{B}_0\mathcal{B}_0\right], \tag{2.10}$$

where $Q_a^i := \frac{1}{2}\varepsilon_{abc}\varepsilon^{ijk}\varphi_j^b\varphi_k^c$, $\varphi := (\zeta, \Theta, \Phi)$ and $a, b, c, i, j, k \in \{1, 2, 3\}$.

Finally, the pion mass term in the standard BPS version of the model (BPSS) $\mathcal{L}_0^{BPSS} = -\mu^2 V$ is taken to involve the potential $V = \frac{1}{2}\text{Tr}(\mathbb{I}-U) = 1 - \cos\zeta$, but we will allow here other forms of the potential as well. Further extensions, including for instance a sextic derivative term [30] or multiplying the terms with field dependent coupling constants [31] have also been studied.

In what follows we shall investigate different combinations of various complex extended or deformed versions of different parts of this model related to the form of $\mathcal{L}$ in (2.1).

3. Pseudo Hermitian variants of Skyrme models

In this section our first guiding principle is to identify a $\mathcal{CPT}$-symmetry in a Hermitian Hamiltonian and extend the model by deforming or adding complex terms to convert it into a non-Hermitian Hamiltonian that still respects this symmetry. Subsequently we try to identify a pseudo Hermitian counterpart in a similar fashion as what is by now standard for non-Hermitian quantum mechanical systems [32,33]. For BPS systems in 1+1 dimensions this approach was recently applied successfully in [27]. We shall now demonstrate that it can also be applied to 3+1 dimensional theories with complex topological solutions.

3.1. Complex boosted BPS Skyrme models

We start with the standard BPS Skyrme model consisting of $\mathcal{L}_6 + \mathcal{L}_0^{BPSS}$ by noting that it remains invariant under the antilinear $\mathcal{CPT}$-transformation: $\zeta \rightarrow -\zeta$, $\iota \rightarrow -\iota$. Thus we may introduce a complex shift in $\zeta \rightarrow \zeta + \iota\kappa$ with $\kappa \in \mathbb{R}$ without breaking that symmetry. We denote here and in what follows the imaginary unit as $\iota := \sqrt{-1}$ to distinguish it from indices i. Choosing $\kappa = -\text{arctanh}\,\epsilon$ with $\epsilon \in \mathbb{R}$ and using the identities $\sqrt{1-\epsilon^2}\sin(\zeta - \iota\,\text{arctanh}\,\epsilon) = \sin\zeta - \iota\epsilon\cos\zeta$, $\sqrt{1-\epsilon^2}\cos(\zeta - \iota\,\text{arctanh}\,\epsilon) = \cos\zeta + \iota\epsilon\sin\zeta$, we obtain a $\mathcal{CPT}$-symmetrically extended BPS Skyrme model of the form

$$\mathcal{L}_b = -\frac{\lambda^2}{4}(\sin\zeta - \iota\epsilon\cos\zeta)^4\sin^2\Theta\,\mathcal{B}_\mu\mathcal{B}^\mu - \mu^2\left(\sqrt{1-\epsilon^2} - \cos\zeta - \iota\epsilon\sin\zeta\right), \qquad (3.1)$$

after re-scaling the coupling constants as $\lambda \rightarrow \lambda(1-\epsilon^2)$, $\mu \rightarrow \mu(1-\epsilon^2)^{1/4}$. By design, for vanishing ϵ the model reduces to the standard BPS Skyrme model $\lim_{\epsilon\to 0}\mathcal{L}_b = \mathcal{L}_6 + \mathcal{L}_0^{BPSS}$ as introduced and discussed in [22]. We shall now demonstrate that the energies for the topological solutions to the equations of motion resulting from $\mathcal{L}_b$ and its corresponding Hermitian counterpart are identical and real.

3.1.1. Topological energies for the real solutions of the Hermitian counterpart

At first we derive the Hamiltonian corresponding to $\mathcal{L}_b$ in the standard fashion by computing the conjugate canonical momenta

$$\Pi^a = \frac{\delta\mathcal{L}_b}{\delta\varphi_0^a} = G_{ac}\varphi_0^c, \quad \text{with } G_{ac} = \frac{\lambda^2}{2}(\sin\zeta - \iota\epsilon\cos\zeta)^4\sin^2\Theta\,Q_a^iQ_c^i, \qquad (3.2)$$

so that

$$\mathcal{H}_b = \frac{1}{2}\Pi^a G_{ac}^{-1}\Pi^c - \mathcal{L}_b, \quad \text{with } G_{ac}^{-1} = \frac{2\varphi_i^a\varphi_i^c}{J^2\lambda^2(\sin\zeta - \iota\epsilon\cos\zeta)^4\sin^2\Theta}, \qquad (3.3)$$

where $J := \frac{1}{2}\varepsilon_{abc}\varepsilon^{ijk}\varphi_i^a\varphi_j^b\varphi_k^c$.

While overall our considerations are mainly classical, we now briefly appeal to the quantum field theoretic version of the model, by assuming the standard canonical equal time commutation relation $\left[\varphi^a(r,t), \Pi^b(r',t)\right] = i\delta^{ab}\delta(r-r')$ between the fields $\varphi^a(r,t)$ and their conjugate momentum operators $\Pi^a(r,t)$. We then use a slightly modified version of the Dyson operator as employed in [34,27]

$$\eta = \exp\left[-\operatorname{arctanh}\epsilon \sum_a \int dx\, \Pi^a(r,t)\right], \tag{3.4}$$

to map the non-Hermitian Hamiltonian functional $\mathcal{H}_b$ to a Hermitian counterpart $\mathfrak{h}_b$ by means of the adjoint action of η

$$\mathfrak{h}_b = \eta \mathcal{H}_b \eta^{-1} = \frac{1}{2}\Pi^a G_{ac}^{-1}\Pi^c + \frac{\tilde{\lambda}^2}{4}\sin^4\zeta\sin^2\Theta\mathcal{B}_\mu\mathcal{B}^\mu + \tilde{\mu}^2(1-\cos\zeta). \tag{3.5}$$

We notice that $\mathfrak{h}_b$ is in fact the standard BPS Skyrme model with reversing the previous re-scaling of the coupling constants as $\lambda \to \tilde{\lambda} = \lambda(1-\epsilon^2)$, $\mu \to \tilde{\mu} = \mu(1-\epsilon^2)^{1/4}$.

In this case the static BPS solution that saturates the Bogomolny bound is known to be computable exactly [22] when using spherical space-time coordinates $(x,y,z) \to (r,\theta,\phi)$ with $r \in [0,\infty)$, $\theta \in [0,\pi)$, $\phi \in [0,2\pi)$ and the identifications $\Theta = \theta$, $\Phi = n\phi$ with $n \in \mathbb{Z}$ together with the assumption that ζ is a function of r only. In this case one obtains a well-defined real compacton solution, see e.g. [35] for what that entails in general,

$$\zeta_r(r) = \begin{cases} 2\arccos\left(\frac{1}{\sqrt{2}}\left|\frac{\tilde{\mu}}{n\tilde{\lambda}}\right|^{1/3} r\right) & \text{for } r \in \left[0, r_c = \sqrt{2}\left|\frac{n\tilde{\lambda}}{\tilde{\mu}}\right|^{1/3}\right] \\ 0 & \text{otherwise} \end{cases}, \tag{3.6}$$

with real energy

$$E = 8\pi\tilde{\mu}^2 \int_0^{r_c} r^2 V[\zeta_r(r)]\, dr = \frac{64}{15}\sqrt{2}\,|n|\,\tilde{\mu}\tilde{\lambda}\pi(1-\epsilon^2)^{5/4}. \tag{3.7}$$

Next we show that there are in fact more solutions in this case and how the same energy results from a direct computation for the complex solution of the non-Hermitian system (3.1).

3.1.2. Energies for the complex solutions of the non-Hermitian system

We adopt here and below the approach proposed in [36], which slightly reformulates the BPS theory and exploits the self-duality and anti-self-duality between certain fields. For this purpose we first note that the Hamiltonian density for static solutions may be expressed as

$$\mathcal{H}_b = A^2 + \tilde{A}^2, \tag{3.8}$$

with

$$A := \frac{\lambda}{2}(\sin\zeta - \imath\epsilon\cos\zeta)^2\sin\Theta\mathcal{B}_0, \qquad \tilde{A} = \mu V = \mu\left(\sqrt{1-\epsilon^2} - \cos\zeta - \imath\epsilon\sin\zeta\right)^{1/2}. \tag{3.9}$$

The self-duality and anti-self-duality between the fields A and $\tilde{A}$

$$A = \pm\tilde{A}, \tag{3.10}$$

is then interpreted as being identical to the BPS equations [20,21]. The energy functional for the solutions of (3.10) therefore acquires the form

$$E_{\mathrm{b}} = \int d^3x \left(A^2 + \tilde{A}^2 \right) = \pm 2 \int d^3x \; A\tilde{A}. \tag{3.11}$$

Note that since the fields A and $\tilde{A}$ are now complex, the energy of the static BPS solutions E_{b} may no longer saturate the Bogomolny bound.

Explicitly the BPS equations (3.10) may be written as

$$\frac{\lambda}{2} \frac{(\sin\zeta - \iota\epsilon\cos\zeta)^2}{\mu\sqrt{V}} \sin\Theta \varepsilon^{ijk} \partial_i\zeta \partial_j\Theta \partial_k\Phi = \pm 1. \tag{3.12}$$

Since $\varepsilon_{ijk}\zeta_i\Theta_j\Phi_k$ is simply the Jacobian for the variable transformation $(x, y, z) \to (\Theta, \Phi, \zeta)$ the multiplication of (3.12) by the volume element d^3x leads to

$$\frac{\lambda}{2} \frac{(\sin\zeta - \iota\epsilon\cos\zeta)^2}{\mu\sqrt{V}} \sin\Theta d\zeta d\Theta d\Phi = \pm r^2 \sin\theta dr d\theta d\phi, \tag{3.13}$$

where we used spherical coordinates on the right hand side. With the same identifications between (r, θ, ϕ) and (ζ, Θ, Φ) as chosen in the previous section and together with the aforementioned trigonometric identities the relation (3.13) converts into

$$\frac{n\tilde{\lambda}}{2r^2} \sin^2(\zeta - \iota\arctanh\epsilon) \frac{d\zeta}{dr} = \pm\tilde{\mu}\sqrt{1 - \cos(\zeta - \iota\arctanh\epsilon)}. \tag{3.14}$$

These equations is easily integrated out by separating variables. Corresponding to the different branches we obtain different types of solutions

$$\zeta_{i,m}^\pm(r) = \tilde{\zeta}_{i,m}^\pm(r) + \iota\arctanh\epsilon = 2\arccos\left[\omega^i \frac{(n\tilde{\lambda}c \mp \tilde{\mu}r^3)^{1/3}}{\sqrt{2}n^{1/3}\tilde{\lambda}^{1/3}} \right] + 2\pi m + \iota\arctanh\epsilon, \tag{3.15}$$

for $i = 0, 1, 2$, $m \in \mathbb{Z}$ and $\omega = e^{2\pi\iota/3}$ denoting the third root of unity. We analytically continue here the arccos-function to the entire complex plane by the well-known formula $\arccos z = -\iota\ln\left(z \pm \sqrt{z^2 - 1}\right)$. Note that for the Hermitian case, i.e. $\epsilon = 0$, all these solutions also arise, but in that case one simply discards the complex solutions or the parts of the solutions that become complex after a certain value of r, by requiring solutions to be real. In order to identify possible compacton solutions in the real part we need to specify the critical values r_0 for which the solution vanish, $\tilde{\zeta}_i^\pm(r_0) = 0$, and also those values r_π for which $\tilde{\zeta}_i^\pm(r_\pi) = \pi$. We obtain

$$r_{0,i}^\pm := \omega^i \left[\frac{\pm n\tilde{\lambda}\left(c - 2^{3/2}\right)}{\tilde{\mu}} \right]^{1/3}, \quad \text{and} \quad r_{\pi,i}^\pm := \omega^i \left(\frac{\pm n\tilde{\lambda}c}{\tilde{\mu}} \right)^{1/3}. \tag{3.16}$$

These values are irrelevant when complex, whereas when real they may produce different types of scenarios depending on their ordering and signs of the constants. In Fig. 1 we depict some interesting possibilities.

It is clear from Fig. 1 that we may construct compacton type solutions in various ways. Obvious choices are

$$\tilde{\zeta}_{\mathrm{BPS}}(r) := \begin{cases} \tilde{\zeta}_{0,0}^- & \text{for } 0 \le r \le r_0^- \\ 0 & \text{for } r_0^- < r \end{cases}, \quad \tilde{\zeta}_{\mathrm{St}}(r) := \begin{cases} \tilde{\zeta}_{1,0}^- & \text{for } 0 \le r \le r_\pi^- \\ \tilde{\zeta}_{0,0}^- & \text{for } r_\pi^- \le r \le r_0^- \\ 0 & \text{for } r_0^- < r \end{cases}. \tag{3.17}$$
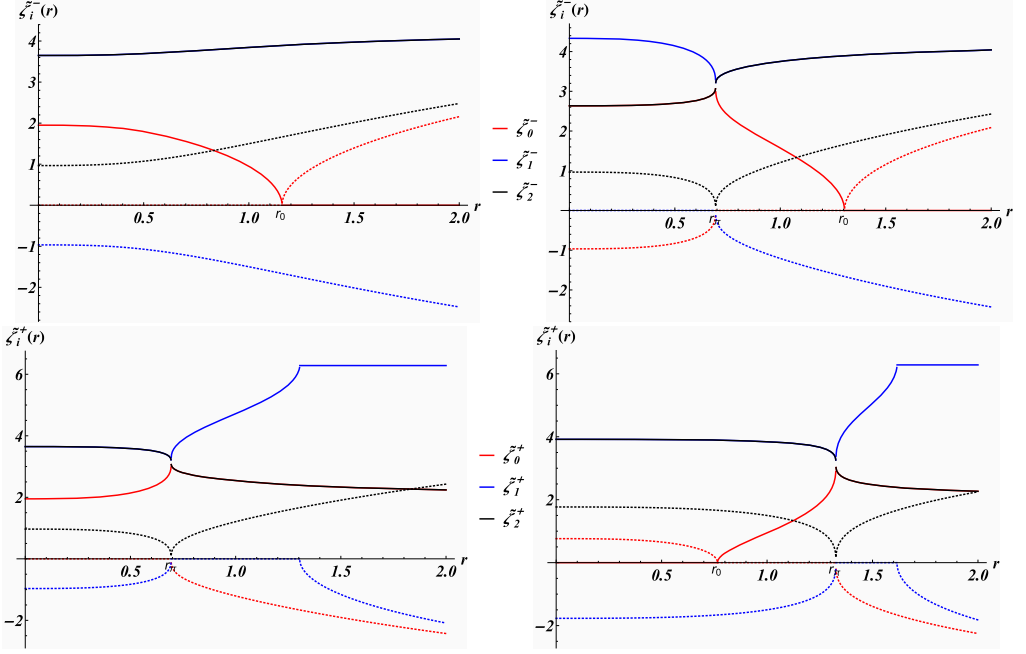
Fig. 1. The $\tilde{\zeta}$-part of the solutions of the BPS equation (3.14) for different scenarios with $n = \tilde{\lambda} = 1$, $\mu = 3/2$ and different choices for c. The different relative orderings are: panel (a) $r_\pi \leq 0 \leq r_0$ with $c = 1/2$, panel (b) $0 \leq r_\pi \leq r_0$ with $c = -1/2$, panel (c) $r_0 \leq 0 \leq r_\pi$ with $c = 1/2$ and panel (d) $0 \leq r_0 \leq r_\pi$ with $c = 7/2$. Real parts correspond to solid lines and imaginary parts to dotted ones.

Noting that $r_{\pi,i}^+(c) = r_{\pi,i}^-(-c)$, we may also glue together solution that are self-dual with those that are anti-self-dual as

$$
\tilde{\zeta}_{\text{Cusp}}(r) := \begin{cases} \tilde{\zeta}_{0,0}^+ & \text{for } 0 \leq r \leq r_\pi^+ = r_\pi^- \\ \tilde{\zeta}_{0,0}^- & \text{for } r_\pi^- \leq r \leq r_0^- \\ 0 & \text{for } r_0^- < r \end{cases},
$$

$$
\tilde{\zeta}_{\text{Shell}}(r) := \begin{cases} 0 & \text{for } r < r_0^+ \\ \tilde{\zeta}_{0,0}^+ & \text{for } r_0^+ \leq r \leq r_\pi^+ = r_\pi^- \\ \tilde{\zeta}_{0,0}^- & \text{for } r_\pi^- \leq r \leq r_0^- \\ 0 & \text{for } r_0^- < r \end{cases}. \tag{3.18}
$$

A purely imaginary compacton solution is obtained as $\tilde{\zeta}_{\text{iBPS}}(r) := \tilde{\zeta}_{0,0}^+$ for $r < r_0^+$ and 0 otherwise. Here and below our terminology is inspired by the radial profile of our solutions. We have dropped the second subscript on $r_{0,i}^\pm$ and $r_{\pi,i}^\pm$ as the branch that produces a real values depends on the values of $\tilde{\lambda}$, $\tilde{\mu}$ and c. It appears that in this way one is combining solutions from different equations. However, noting that the equation of motion resulting from (3.1) is simply the square of the BPS equations (3.14), see e.g. [22] for a derivation when $\epsilon = 0$, we adopt here the view that the latter is more fundamental. Hence, we are combining solutions for one single equation with different choices of integration constants in different domains. Whilst the first order derivative are discontinuous at the 'gluing points' $r_0^\pm$ and $r_\pi^\pm$ in the solutions in (3.17) and (3.18), we may argue here in a similar way as in [22] to establish that the solutions are in fact well defined
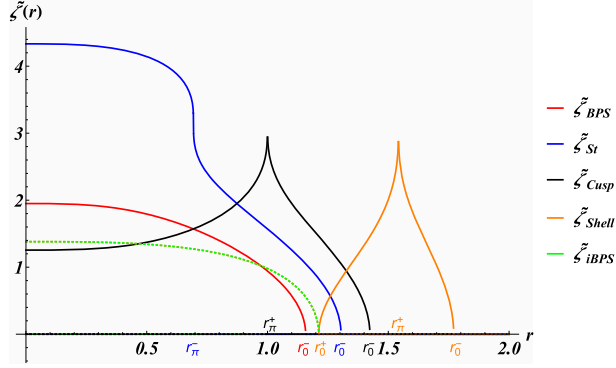
Fig. 2. The BPS solution $\tilde{\zeta}_{\text{BPS}}$ with $n = 1$, $c = 1/2$, $\tilde{\mu} = 3/2$, $\tilde{\lambda} = 1$, the step solution $\tilde{\zeta}_{\text{St}}$ with $n = 1$, $-c = 1/2$, $\tilde{\mu} = 3/2$, $\tilde{\lambda} = 1$, the cusp solution $\tilde{\zeta}_{\text{Cusp}}$ with $n = 1$, $c = 3/2$, $\tilde{\mu} = 3/2$, $\tilde{\lambda} = 1$, the shell solution $\tilde{\zeta}_{\text{Shell}}$ with $n = 1$, $c = 11/2$, $\tilde{\mu} = 3/2$, $\tilde{\lambda} = 1$ and the purely imaginary solution $\tilde{\zeta}_{\text{iBPS}}$ with $n = 1$, $c = 11/2$, $\tilde{\mu} = 3/2$, $\tilde{\lambda} = 1$. (For interpretation of the colours in the figure(s), the reader is referred to the web version of this article.)
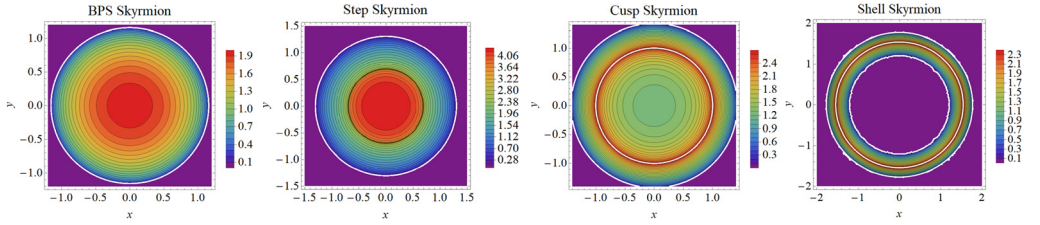

Fig. 3. Different types of solutions to the equations of motion as defined in (3.18) - (3.17) with parameters $n = \tilde{\lambda} = 1$, $\tilde{\mu} = 3/2$ and $c = 1/2$ in panel (a), $c = -1/2$ in panel (b), $c = 3/2$ in panel (c), $c = 11/2$ in panel (d).

solutions. The derivative $d\tilde{\zeta}/dr$ always occurs multiplied with a $\sin^2 \tilde{\zeta}$ in the BPS equations, so that the left and right limits of this combination is always finite at the gluing points, but might differ by a sign. Since this sign is irrelevant in the equations of motion the solutions are well defined and lead to meaningful values for the energy density and the Baryon number density. We depict the configurations (3.18) - (3.17) in Fig. 2.

In Fig. 3 we present the Skyrmion solutions of compacton type (3.18) - (3.17) as slices in form of level curves. We may compare with Fig. 2. In panel (a) we have a standard real (fractional) Skyrmion $\tilde{\zeta}_{\text{BPS}}$ starting at a finite value at $r = 0$ and then decaying to zero at some critical value r_0^-. In panel (b) we depict the solution $\tilde{\zeta}_{\text{St}}$ taking on the form of a step like function with an inflection point at r_π^-. The solution $\tilde{\zeta}_{\text{Cusp}}$ shown in panel (c) has a discontinuous first order derivative at $r = r_\pi^+ = r_\pi^-$, which is usually referred to as peakons in the context of 1+1 dimensional integrable systems. The most interesting structure $\tilde{\zeta}_{\text{Shell}}$ is seen in panel (d), which corresponds to a real shell with a peakon structure. We may even change this solution in the region $r < r_0^+$, by defining it as $\tilde{\zeta}_{\text{Core}}(r) = \tilde{\zeta}_{0,0}^+$ for $r < r_0^+$, hence adding a purely imaginary core to it. It turns out that this is consistent as the core has also real energies despite the fact that it is complex.

Next we demonstrate that all types of solutions depicted in Figs. 2 and 3 possess real energies. We compute these energies on some domain $r \in [\tilde{r}_c, r_c]$ by using the general expression (3.11)

$$E = \pm \tilde{\lambda} \tilde{\mu} \int d^3x \, (\sin \zeta - \iota \epsilon \cos \zeta)^2 \sin \Theta \mathcal{B}_0 \left(\sqrt{1 - \epsilon^2} - \cos \zeta - \iota \epsilon \sin \zeta \right)^{1/2} \tag{3.19}$$

$$= \pm 4\pi \tilde{\lambda} \tilde{\mu} n \int_{\tilde{r}_c}^{r_c} dr \sin^2 (\zeta(r) - \iota \operatorname{arctanh} \epsilon) \sqrt{1 - \cos (\zeta(r) - \iota \operatorname{arctanh} \epsilon)} \frac{d\zeta}{dr} \tag{3.20}$$

$$= 8\pi \tilde{\mu}^2 \int_{\tilde{r}_c}^{r_c} dr \, r^2 V [\zeta(r)]. \tag{3.21}$$

In the last step we used once more equation (3.14). For the solutions $\tilde{\zeta}_{\text{BPS}}$, $\tilde{\zeta}_{\text{St}}$ and $\tilde{\zeta}_{\text{Cusp}}$ we calculate

$$E_{\text{BPS/St,Cusp}} = \frac{8}{15} n \tilde{\mu} \tilde{\lambda} \pi \left(8\sqrt{2} \mp 10c \pm 3c^{5/3} \right), \tag{3.22}$$

for $c \geq 0$ on the domains as indicated in Fig. 1. The upper signs stand here for BPS and lower signs for the step and cusp solutions, which have the same energies. As expected, the expressions (3.22) reduce to the energy of the standard real case (3.7) in the limit $c \to 0$, since in that case the fractional BPS Skyrmions become full BPS Skyrmions with $\zeta(r = 0) = \pi$. For the shell solution $\tilde{\zeta}_{\text{Shell}}$ and the purely imaginary core solution $\tilde{\zeta}_{\text{iBPS}}$ we obtain the real energies

$$E_{\text{Shell}} = \frac{128}{15} \sqrt{2} n \tilde{\mu} \tilde{\lambda} \pi, \quad \text{and} \quad E_{\text{iBPS}} = -E_{\text{BPS}}, \tag{3.23}$$

respectively. The reality of the solutions is ensured by verifying that the respective solutions satisfy all three conditions (1.1)-(1.3) for a particular $\mathcal{CPT}'$-symmetry. With condition (1.1) we identify here the symmetry to

$$\mathcal{CPT}' : \zeta(x_\mu) \to \zeta^*(-x_\mu) + 2\iota \operatorname{arctanh} \epsilon = \zeta(-x_\mu). \tag{3.24}$$

We are considering static solutions in which the angle dependence has already been eliminated, so that our solutions only depend on r. Hence the change in the arguments of the fields $x_\mu \to -x_\mu$ is automatically satisfied. The $\mathcal{CPT}'$-symmetry condition (3.24) is then easily verified for our solutions $\zeta_{i,m}^{\pm}(r)$ in (3.15): $\zeta_{i,m}^{\pm}(r) \to \left[\zeta_{i,m}^{\pm}(r) \right]^* + 2\iota \operatorname{arctanh} \epsilon = \zeta_{i,m}^{\pm}(r)$. Since the solutions are mapped to themselves, the condition (iii) is automatically satisfied and energies for these solutions must be real. Notice that the symmetry $\mathcal{CPT}'$ differs from the symmetry $\mathcal{CPT}$ we used for the construction of the model.

Apart from ζ_{iBPS}, the solutions of the Hermitian theory in this section are all real and given the above argument their corresponding energies therefore saturate the lower Bogomolny bound. However, we note that ζ_{iBPS} is nonphysical since its corresponding energy is not bounded from below. This is either seen from (3.23) or more generally from (3.11), which implies that for purely imaginary A and $\tilde{A}$ the right hand side constitutes an upper bound for the energy.

We conclude this section with a brief comment on the values for the Baryon number, that in general is no longer integer valued. Taking the normalization constant to be $N_0 = 24\pi^2$ we obtain

$$B = \int B_0 d^3x = \frac{n}{\pi} \left[\zeta^{\pm}(r = 0) - \frac{1}{2} \sin \left[2\zeta^{\pm}(r = 0) \right] \right], \tag{3.25}$$

which is no longer integer valued. However, choosing N_0 differently we can always ensure that the Baryon number is integer valued.

It is worth pointing out that we may reach similar conclusions as in the boosted model discussed in this section for a model with complex rotated fields. With a slight modification of the
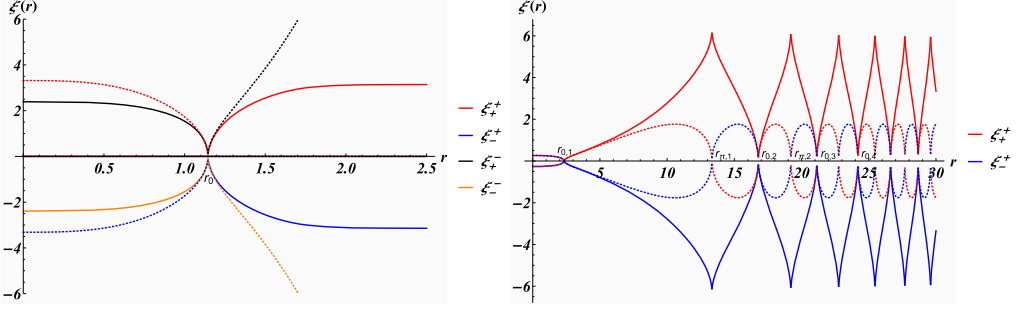
Fig. 4. Panel (a): Purely imaginary and real compacton and semi-kink solutions (4.3) resulting from the potential $V_{SK}(\zeta)$ with parameter choices $n = \lambda = 1$, $\mu = 2$ and $c = \pm 1$ for $\gamma = \mp 1$. Panel (b): Complex solutions with zero energy resulting from the potential $V_{m0}(\zeta)$ with parameter choices $n = \lambda = 10$, $\mu = 2$ and $c = \pm 25.15$ for $\gamma = \mp 1$. Real parts correspond to solid lines and imaginary parts to dotted ones.

Dyson map used in [39], having the effect on the fields is that they transform as $\varphi^a \to e^{-i\theta_a} \varphi^a$ and $\Pi^a \to e^{i\theta_a} \Pi^a$, we may construct a new complex models. The model obtained in this manner also possess complex BPS solutions with real energies.

4. Skyrme model with semi-kink and massless solutions

While most Skyrmion solutions are of compacton type, there exist also interesting variants of the model $\mathcal{L}_0 + \mathcal{L}_6$ with potentials that lead to solutions which are partly of kink type with real energies. We consider here the potential

$$V_{SK}(\zeta) = \sin^2 \zeta (1 + \cos \zeta)^2. \tag{4.1}$$

The corresponding BPS equations

$$\tan\left(\frac{\zeta}{2}\right) \frac{d\zeta}{dr} = \pm \frac{2\mu}{n\lambda} r^2, \tag{4.2}$$

are easily solved to

$$\zeta_s^\pm(r) = 2s \ \arccos\left(e^{\mp \frac{\mu r^3}{3n\lambda} - c}\right), \tag{4.3}$$

with $s = \pm 1$ and c denoting an integration constant. A similar solutions to $s = 1$ was found in [24]. Evidently we have $\zeta_s^\pm(r_0^\pm) = 0$ for $r_{0,i}^\pm = \omega^i (\mp 3n\lambda c/\mu)^{1/3}$ and asymptotically $\zeta_s^\pm$ acquires a finite value $\lim_{r\to\infty} \zeta_s^\pm(r) = s\pi$ for $\pm\mu/n\lambda > 0$. We depict some sample solutions in Fig. 4 panel (a). For $r < r_0$ we notice the previously observed standard real or purely imaginary compacton solutions, but for $r > r_0$ the solutions $\zeta_\pm^+$ exhibit the interesting feature of being of compacton type at $r = r_0$ and of kink type when $r \to \infty$.

Crucially, it turns out that the energies of these solutions are all real and finite. From the general expression (3.21) we compute

$$E_{\text{semi-kink}}\left(\zeta_s^-\right) = \frac{16n\lambda\mu\pi}{3}, \tag{4.4}$$

$$E_{\text{real compacton}}\left(\zeta_s^-\right) = -\left(4e^{-6c} - 3e^{-8c} - 1\right) E_{\text{semi-kink}}, \tag{4.5}$$

$$E_{\text{purely imaginary compacton}}\left(\zeta_s^+\right) = \left(4e^{6c} - 3e^{8c} - 1\right) E_{\text{semi-kink}}, \tag{4.6}$$

for $c > 0$ and $n\lambda\mu > 0$.

Another interesting variant emerges when considering the potential $V_{m0}(\zeta) = -V_{SK}(\zeta)$. In this case the solutions become $\check{\zeta}_s^{\pm}(r) = 2s \arccos(e^{\mp\iota \frac{\mu r^3}{3n\lambda} - \iota c})$, which vanish for $r_{0,i}^{\pm} = \omega^i(\mp 3n\lambda(c + 2\pi m)/\mu)^{1/3}$ with $m \in \mathbb{Z}$ and $\check{\zeta}_s^{\pm}(r_{\pi,i}^{\pm}) = 2\pi s$ for $r_{\pi,i}^{\pm} = \omega^i[\mp 3n\lambda(c + 2\pi(m + 1/2))/\mu]^{1/3}$. A sample solution is depicted in Fig. 4 panel (b). We observe a re-occurring complex periodic shell solution that becomes squeezed for increasing r. Interestingly the energies for these type of shell solutions is vanishing

$$8\pi\mu^2 \int_{r_0^+}^{r_0^-} dr\, r^2 V_{m0}\left[\check{\zeta}_s^{\pm}(r)\right] = 0. \tag{4.7}$$

This suggests that the shell solutions may be interpreted as massless Skyrmions.

We observe from (1.3) that the energies of the solutions are ensured to be real by the $\mathcal{CPT}_{\pm}$-symmetries: $\zeta(r) \to \pm\zeta^*(r)$. For the same reasons as in the previous subsection there is no effect on the arguments of the fields. For the complex solution $\check{\zeta}_s^{\pm}$ this reads $\mathcal{CPT}_{\pm}$: $\zeta_s^{\pm}(c) \to \left[\zeta_{\pm s}^{\pm}(c)\right]^* = \zeta_{\pm s}^{\mp}(-c)$. Thus in this case this $\mathcal{CPT}_{\pm}$-symmetries map solutions to different solutions. However, invoking condition (1.3) and noting that the energies for $\check{\zeta}_s^{\pm}(r)$ are the same for both BPS equations and independent of s, c, they must be real.

5. Skyrme model with a Bender-Boettcher type potential

We will now investigate further variants of the model $\mathcal{L}_0 + \mathcal{L}_6$ by allowing for a wider range of potentials in $\mathcal{L}_0$, including the possibilities of functions of $\text{Tr}\,[U(\zeta)]$ and even $\text{Tr}\,[U(\iota\zeta)]$. As a first example we consider the potential

$$V_{BB}(\zeta) = (\iota\zeta)^{\varepsilon} \sin^4 \zeta, \quad \varepsilon \in \mathbb{R}. \tag{5.1}$$

This potential closely resembles the classical prototype potential studied in $\mathcal{PT}$-symmetric quantum mechanics [40], remaining invariant under the $\mathcal{CPT}$-transformation: $\zeta \to -\zeta$, $\iota \to -\iota$. Using the same parameterization and reasonings as in the previous sections, the BPS equations derived in analogy to (3.14) read

$$\frac{n\lambda}{2\mu} \frac{\sin^2(\zeta)}{\sqrt{V_{BB}}} d\zeta = \pm r^2 dr \quad \Rightarrow \quad \frac{d\zeta}{dr} = \pm\frac{2\mu}{n\lambda}(\iota\zeta)^{\varepsilon/2} r^2. \tag{5.2}$$

These equations are easily integrated, acquiring the following Gaussian form

$$\zeta_m^{\pm}(r) = \left[\left|\frac{n\lambda}{\mu(\varepsilon - 2)}\right| \frac{1}{(c + r^3/3)}\right]^{\frac{2}{\varepsilon - 2}} e^{\iota\pi\left(\frac{3s}{2-\varepsilon} - \frac{1}{2}\right)} e^{2\pi\iota \frac{2m}{\varepsilon - 2}}, \quad s = \pm 1, c \in \mathbb{R}, m \in \mathbb{Z}. \tag{5.3}$$

In principle the integration constant c could be complex, but we only obtain real energies for $c \in \mathbb{R}$ so we ignore that possibility in what follows. We have defined the constant $s := \text{sign}[\pm n\lambda/\mu(\varepsilon - 2)]$ where as above sign denotes the signum function. The last factor accounts for all the branches of ζ, as can either be seen by inserting $1 = e^{2\pi\iota m}$ into the square bracket or by noting that $\zeta \to \zeta e^{2\pi\iota \frac{2m}{\varepsilon - 2}}$ is a symmetry of equation (5.2). The BPS solutions $\zeta_m^{\pm}(r)$ exhibit two different types of qualitative behaviour. When $c \in \mathbb{R}^-$, $\varepsilon < 2$ we obtain compacton solutions with finite values at $r = 0$ and $\zeta_m^{\pm}[(3|c|)^{1/3}] = 0$. For $c \in \mathbb{R}^+$, $\varepsilon > 2$ the solutions are finite at $r = 0$ and tend to zero only for $r \to \infty$. We illustrate these types of behaviour in Fig. 5.
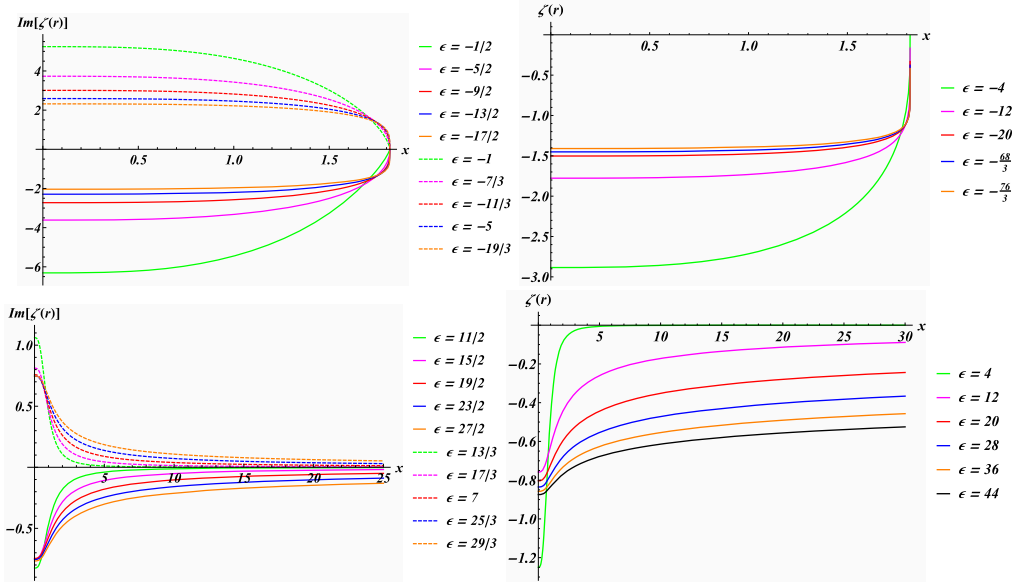
Fig. 5. BPS solutions $\zeta_m^{\pm}(r)$ for a Skyrme model with a Bender-Boettcher type potential for the parameter choices $\lambda = 1$, $\mu = 2$, $n = 1$. In panels (a), (b) we have taken $c = -2$ and in panels (c), (d) we have $c = 0.2$.

By the same reasoning as in the previous subsections the energies for these solutions are computed to

$$E_{\mathrm{BB}}^{\pm} = 8\pi\mu^2 \int_0^{r_c} dr r^2 V\left[\zeta_m^{\pm}(r)\right], \tag{5.4}$$

where $r_c = (3|c|)^{1/3}$ for the compacton solutions and $r_c \to \infty$ for the unbounded ones. As is evident from (5.1) these energies can be real when ζ is either purely imaginary or real. Together with (5.3) real energies are found when

$$\zeta \in -\imath\mathbb{R}^+: \quad \varepsilon = \frac{4m + 4\ell - 3s}{2\ell}, \quad \ell, m \in \mathbb{N}, \tag{5.5}$$

$$\zeta \in \imath\mathbb{R}^+: \quad \varepsilon = \frac{2 + 4m + 4\ell - 3s}{1 + 2\ell}, \quad m, \varepsilon \in \mathbb{N}, \ell \in \mathbb{N}_0, \tag{5.6}$$

$$\zeta \in \mathbb{R}: \quad \varepsilon = \frac{2(1 + 4m + 2\ell - 3s)}{1 + 2\ell}, \quad \ell, m \in \mathbb{N}_0, \ell, \varepsilon \in 4\mathbb{N}. \tag{5.7}$$

Examples for these solutions are depicted in Fig. 5. In panel (b) of that figure we also displayed a two solution real solutions with $\varepsilon \notin 4\mathbb{N}$. Next we plot the corresponding energies for these cases as functions of ε in Fig. 6.

We observe from Fig. 6 that the energies are finite and follow distinct curves for the different cases. Moreover, for the case $\zeta \in -\imath\mathbb{R}^+$ the curve is fairly dense and becomes more connected when including more values for ℓ and m, hence ε. In the other cases this can not be achieved due to the additional restriction on ε so that the distribution is more sparse. The transition at $\varepsilon = 2$ is not smooth.

For these models the $\mathcal{CPT}'$-symmetry identified from (1.3) must act as $\zeta \to -\zeta^*$. For our solutions in (5.3) this becomes $\zeta_m^{\pm} \to -(\zeta_m^{\pm})^* = \zeta_{-m}^{\mp}$. Noting now that $\varepsilon(m, \ell, s) = \varepsilon(-m, -\ell, -s)$
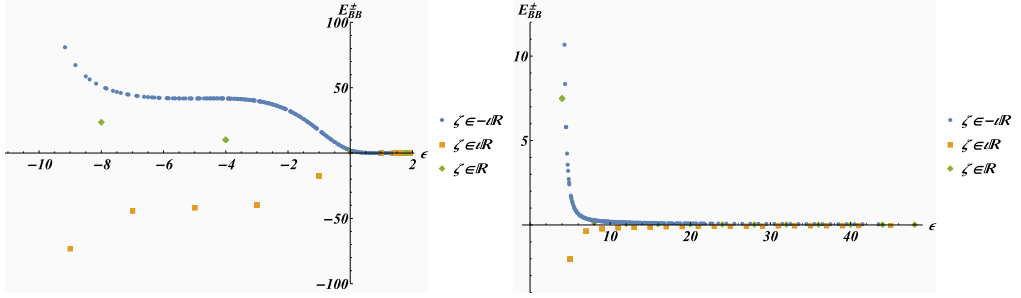
Fig. 6. Real energies $E_{\bar{B}B}^{\pm}$ of the compacton (panel a) and unbounded (panel b) BPS solutions for the cases (5.5) - (5.7) with $\lambda = 1$, $\mu = 2$, $n = 1$ and $c = 0.2$ for several values of ℓ, m.

in (5.5) and $\varepsilon(m, \ell, s) = \varepsilon(-m, -\ell - 1, -s)$ in (5.6), (5.7), we simply have to choose a new $\ell' = -\ell$, $\ell' = -\ell - 1$, respectively, to obtain the same value for ε. This establishes that $E[\zeta_m^{\pm}] = E[\zeta_{-m}^{\mp}]$ so that condition (iii) in (1.3) also holds and the energy must therefore be real. Notice once more that the $\mathcal{CPT}'$-symmetry that ensures the reality of the energies is different from $\mathcal{CPT}$, that was observed initially for $V_{BB}(\zeta)$.

6. Skyrme model with complex trigonometric potentials

Next we study a model for which the Hamiltonian respects again the $\mathcal{CPT}$-symmetry: $\zeta \to -\zeta$, $\iota \to -\iota$, but which has solutions transforming under a $\mathcal{CPT}'$-symmetry to satisfy (1.1) with conditions (1.2) and/or (1.3) violated. Thus we are in the broken $\mathcal{CPT}'$-regime. For this purpose we consider the variant of the model $\mathcal{L}_0 + \mathcal{L}_6$ involving the trigonometric potential

$$V_T(\zeta) = \sin^4 \zeta \cos^4(\zeta + i\epsilon), \quad \varepsilon \in \mathbb{R}. \tag{6.1}$$

We notice that unlike as in the pseudo Hermitian model discussed in section 3 only one of the factors in the potential is shifted so that the potential is not simply boosted and most likely not pseudo Hermitian. The BPS equations take the form

$$\frac{n\lambda}{2\mu} \frac{\sin^2 \zeta}{\sqrt{V_T}} d\zeta = \pm r^2 dr \quad \Rightarrow \quad \frac{d\zeta}{dr} = \pm 3\alpha \cos^2(\zeta + i\epsilon) r^2, \tag{6.2}$$

where we abbreviated $\alpha := \frac{2\mu}{3n\lambda}$. Integrating this equation we find the solutions

$$\zeta_{\alpha,\gamma}^{\pm}(r) = -i\epsilon \pm \arctan \alpha(r^3 + \gamma), \tag{6.3}$$

with integration constant $\gamma \in \mathbb{C}$. The symmetry identified from condition (i) in (1.1) acts as $\mathcal{CPT}'$: $\zeta_{\alpha,\gamma}^{\pm} \to -\left(\zeta_{\alpha,\gamma}^{\pm}\right)^* = \zeta_{\alpha,\gamma}^{\mp}$. Thus the second condition (1.2) still holds. However, the energies of the two solutions related in this manner are in general not degenerate, i.e. $E[\zeta_{\alpha,\gamma}^{+}] \neq E[\zeta_{\alpha,\gamma}^{-}]$. Depending on the nature of the integration constant γ we find two different types of behaviour and we can still find discrete values for the two $\mathcal{CPT}'$ related solutions that have degenerate energies.

6.1. Real integration constants $\gamma \in \mathbb{R}$

Computing the energy $E_{\alpha,\gamma}^{\pm}$ as in the previous sections, the real and imaginary part acquire the form

$$\operatorname{Re} E_{\alpha,\gamma}^{\pm} = \frac{1}{32} \left(\frac{\pi}{\alpha} - \frac{2\gamma}{\alpha^2\gamma^2+1} \right)$$

$$+ \frac{1}{48} \left(\frac{2\gamma\left(\alpha^2\gamma^2+3\right)}{\left(\alpha^2\gamma^2+1\right)^2} - \frac{\pi}{\alpha} \right) \cosh 2\epsilon + \frac{\gamma\left(\alpha^2\gamma^2-3\right)\cosh 4\epsilon}{72\left(\alpha^2\gamma^2+1\right)^3}$$

$$+ \frac{\gamma\left(2\cosh 2\epsilon - 3\right)}{48\alpha} \arctan\alpha\gamma , \tag{6.4}$$

$$\operatorname{Im} E_{\alpha,\gamma}^{\pm} = \mp \frac{\sinh 2\epsilon\left(\left[3\alpha^2\gamma^2-1\right]\cosh(2\epsilon)+3+3\alpha^2\gamma^2\right)}{36\alpha\left(\alpha^2\gamma^2+1\right)^3}. \tag{6.5}$$

This in general the energy is complex and we have $E_{\alpha,\gamma}^{+} = \left(E_{\alpha,\gamma}^{-}\right)^{*}$ and the model is in the broken $\mathcal{CPT}'$-phase. However, we note that the imaginary part vanishes when parameterizing the integration constant as

$$\gamma_\ell(\alpha,\epsilon) = \ell\operatorname{sech}\epsilon\frac{\sqrt{\cosh 2\epsilon - 3}}{\sqrt{6}\alpha}, \qquad \ell = \pm. \tag{6.6}$$

In this case we have also satisfied condition (iii) in (1.3) with $E[\zeta_{\alpha,\gamma}^{+}] = E[\zeta_{\alpha,\gamma}^{-}]$ and the $\mathcal{CPT}'$-symmetry is restored. In order to keep the condition $\gamma \in \mathbb{R}$, we must restrict $|\epsilon| \in [\frac{1}{2}\operatorname{arccosh} 3, \infty)$.

6.2. Purely imaginary integration constants $\gamma \in i\mathbb{R}$

Taking now γ to be purely imaginary the $\mathcal{CPT}'$-symmetry acts as $\mathcal{CPT}': \zeta_{\alpha,\gamma}^{\pm} \to -\left(\zeta_{\alpha,\gamma}^{\pm}\right)^{*} = \zeta_{\alpha,-\gamma}^{\mp}$. The real and imaginary parts of the energies become now

$$\operatorname{Re} E_{\alpha,\gamma}^{\pm} = \frac{\pi}{32\alpha} \left(1 - \frac{2}{3}\cosh 2\epsilon \right), \tag{6.7}$$

$$\operatorname{Im} E_{\alpha,\gamma}^{\pm} = \pm \frac{\sinh 2\epsilon\left(\left[1+3\alpha^2\gamma^2\right]\cosh 2\epsilon - 3 + 3\alpha^2\gamma^2\right)}{36\alpha\left(1-\alpha^2\gamma^2\right)^3} + \gamma\frac{\left(2\cosh 2\epsilon - 3\right)}{48\alpha}\arctan\alpha\gamma$$

$$- \frac{\gamma}{72}\frac{\left(\alpha^2\gamma^2+3\right)\cosh 4\epsilon + \left(1-\alpha^2\gamma^2\right)\left(3-\alpha^2\gamma^2\right)\cosh 2\epsilon}{(1-\alpha^2\gamma^2)^3}. \tag{6.8}$$

Interestingly the real part becomes very simple and does not depend on the integration constant γ. We may, however, still find values for γ as function of α and ϵ for which the imaginary part (6.8) vanishes, but not in a closed form as in (6.6). In this case condition (iii) in (1.3) becomes $E[\zeta_{\alpha,\gamma}^{+}] = E[\zeta_{\alpha,-\gamma}^{-}]$ and the $\mathcal{CPT}'$-symmetry is also restored.

7. A new Skyrme submodel with complex BPS solutions and real energy

By decomposing the sigma model and the Skyrme term, Adam, Sanchez-Guillen and Wereszczynski noticed in [41] that one may define further consistent and solvable submodels by combining terms from either decomposition as

$$\mathcal{L}_{+}^{(1)} := \mathcal{L}_{2}^{(1)} + \mathcal{L}_{4}^{(1)}, \quad \text{and} \quad \mathcal{L}_{+}^{(2)} := \mathcal{L}_{2}^{(2)} + \mathcal{L}_{4}^{(2)}.$$

Choosing the coupling constant in front of $\mathcal{L}_4$ to be negative relative to $\mathcal{L}_2$, we consider now a slight modification of the second submodel defined by the Lagrangian densities

$$\mathcal{L}_-^{(2)} := \lambda\left(\mathcal{L}_2^{(2)} - \mathcal{L}_4^{(2)}\right), \quad \lambda \in \mathbb{C}. \tag{7.1}$$

The corresponding Hamiltonian density for static solutions may then be written as

$$\mathcal{H}_-^{(2)} = \lambda(\nabla\zeta)^2 - \lambda \sin^4\zeta \sin^2\Theta\,(\nabla\Theta \times \nabla\Phi)^2 = A^2 + \tilde{A}^2, \tag{7.2}$$

where the dual fields are defined as

$$A_i = \sqrt{\lambda}\zeta_i, \qquad \text{and} \qquad \tilde{A}_i = \iota\sqrt{\lambda}\sin^2\zeta \sin\Theta\varepsilon_{ijk}\Theta_j\Phi_k. \tag{7.3}$$

Thus, the Hamiltonian density is of the same generic form as for the class of general BPS models discussed in [36]. Hence, following the same reasoning, the imposition of a self-duality and anti-self-duality between A_i and $\tilde{A}_i$,

$$A_i = \pm\tilde{A}_i \tag{7.4}$$

selects out the BPS equations [20,21]. Thus the energy functional $E_-^{(2)}$ for the solutions of (7.4) therefore acquires the form as in equation (3.11).

We now solve the BPS equations (7.4) and subsequently compute the energies $E_-^{(2)}$ for the solutions obtained. Multiplying (7.4) by Θ_i, Φ_i, ζ_i and summing over i we obtain the respective equations

$$\zeta_i\Theta_i = 0, \quad \zeta_i\Phi_i = 0, \quad \text{and} \quad \zeta_i\zeta_i = \pm\iota \sin^2\zeta \sin\Theta\varepsilon_{ijk}\zeta_i\Theta_j\Phi_k. \tag{7.5}$$

The first two constraints are satisfied by a suitable choice of the space-time dependence of Θ, Φ, ζ. Since $\varepsilon_{ijk}\zeta_i\Theta_j\Phi_k$ is simply the Jacobian for the variable transformation $(x, y, z) \rightarrow (\Theta, \Phi, \zeta)$, the multiplication of the last equation by the volume element d^3x in (7.5) leads to

$$(\nabla\zeta)^2 d^3x = \pm\iota \sin^2\zeta \sin\Theta d\Theta d\Phi\,d\zeta. \tag{7.6}$$

Similarly as above, we choose spherical space-time coordinates $(x, y, z) \rightarrow (r, \theta, \phi)$ with $r \in [0, \infty)$, $\theta \in [0, \pi)$, $\phi \in [0, 2\pi)$, identify $\Theta = \theta$, $\Phi = n\phi$ with $n \in \mathbb{Z}$ and assume $\zeta(r) \in \mathbb{C}$. These choices will automatically solve the first two equations in (7.5), whereas the last one reduces to

$$\frac{d\zeta}{dr} = \pm\iota\frac{n}{r^2}\sin^2\zeta. \tag{7.7}$$

Apart from the ι, this equation coincides with equation (3.6) in [41] derived for $\mathcal{L}_+^{(2)}$ by expressing the unit vector $\vec{n}$ by means of a stereographic projection. We solve equation (7.7) to

$$\zeta_\pm^{(m)}(r) = \iota\,\text{arccoth}\left(c \mp \frac{n}{r}\right) + m\pi, \qquad c \in \mathbb{C}, m \in \mathbb{Z}. \tag{7.8}$$

As seen in Fig. 7 the imaginary parts of these solutions tend to zero for $r \rightarrow \infty$, whereas the real parts approach asymptotically the constant value $m\pi + \tilde{c}/2$ when taking $c = \iota\cot(\tilde{c}/2)$, $\tilde{c} \in \mathbb{R}\backslash\{2n\pi\}$ with $n \in \mathbb{Z}$. Moreover $\lim_{r\rightarrow 0}\zeta_\pm^{(m)}(r) = m\pi$.

At first sight the solution (7.8) may seem to be unattractive due to its complex nature. However, first of all it is continuous throughout the entire range of r and thus overcomes an issue of the real solutions $\zeta_r^{(m)} = \text{arccot}\left(c - \frac{n}{r}\right) + m\pi$ found for $\mathcal{L}_+^{(2)}$ in [41], which are discontinuous at $r = n/c$. Moreover the energies for these solutions are real. We compute
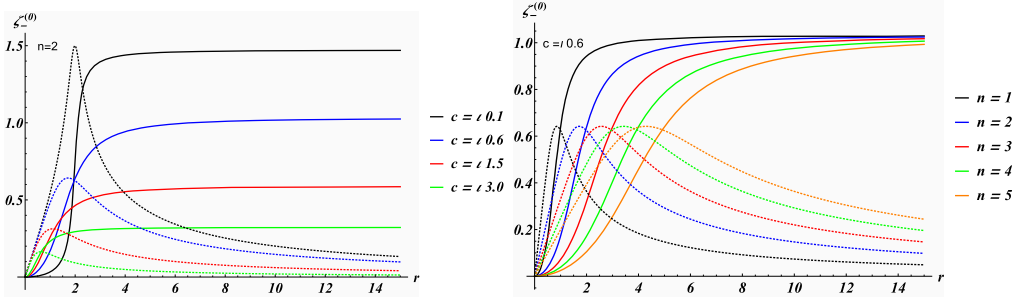
Fig. 7. Complex BPS solutions $\zeta_-^{(0)}$ for different values of n and the initial condition c for $\mathcal{L}_-^{(2)}$. Real parts as solid and imaginary parts as dotted lines.

$$E_-^{(2)}(\zeta) = \pm 2\iota\lambda \int d^3x \, \sin^2\zeta \, \sin\Theta \varepsilon_{ijk}\zeta_i \Theta_j \Phi_k \tag{7.9}$$

$$= \pm 2\iota n\lambda \int \sin^2\zeta \, \sin\theta d\theta d\phi \, d\zeta$$

$$= \pm 8\pi\iota n\lambda \int_0^\infty \sin^2\zeta \frac{d\zeta}{dr} dr$$

$$= \pm 8\pi\iota n\lambda \int_{\zeta(0)}^{\zeta(\infty)} \sin^2\zeta d\zeta = \pm 2\pi\iota n\lambda \left[2\zeta - \sin(2\zeta)\right]\big|_{\zeta(0)}^{\zeta(\infty)}. \tag{7.10}$$

Thus taking now the complex coupling constant to be of the form $\lambda = \iota\tilde{\lambda}$, $\tilde{\lambda} \in \mathbb{R}$, we obtain for solutions $\zeta_\pm^{(m)}$ the real energies

$$E_-^{(2)}\left(\zeta_\pm^{(m)}\right) = \pm 2\pi n\tilde{\lambda}\left[\sin(\tilde{c}) - \tilde{c}\right]. \tag{7.11}$$

We identify the $\mathcal{CPT}$-symmetry from (7.2) as $\mathcal{CPT} : \zeta \to \zeta^*$, which for our solution (7.8) becomes $\zeta_\pm^{(m)}(\tilde{c}) \to \left[\zeta_\pm^{(m)}(\tilde{c})\right]^* = \zeta_\mp^{(-m)}(-\tilde{c})$. Since $E_-^{(2)}\left[\zeta_\pm^{(m)}(\tilde{c})\right] = E_-^{(2)}\left[\zeta_\mp^{(-m)}(-\tilde{c})\right]$, the energies are guaranteed to be real by the antilinear symmetry $\mathcal{CPT}$.

8. Conclusions

We have studied several variants of the Skyrme Lagrangian density $\mathcal{L}$ in equation (2.1). Our main focus has been on finding complex solutions to the self-dual and anti-self-dual versions of the BPS-equation or equation of motion. Identifying the $\mathcal{CPT}$-symmetries for these models from the requirement in (1.1) allowed us to check the remaining conditions (ii), (iii) in (1.2), (1.3) for the constructed solutions, which when satisfied ensures the reality of the energy. The broken $\mathcal{CPT}$-regime was also investigated by providing a sample model in section 7 that is not pseudo Hermitian possessing generic solutions for which neither of the conditions (ii) or (iii) holds. However, when taking the integration constant to be real or purely imaginary and parameterizing it in terms of the coupling constants of the model the reality of the energy could be restored, which is also reflected in the restored $\mathcal{CPT}$-symmetry of the model.

We found a number of novel Skyrmion configurations. Besides the standard compacton or fractional compacton shapes of the BPS-Skyrmions, we found new types of configurations such as complex kink, anti-kink, semi-kink, massless solutions and purely imaginary compactons.

For the model treated in section 3 we have demonstrated that the solutions are mapped to standard solutions for BPS Skyrmion models. This was possible as in that case the explicit Dyson map was constructed. We showed that in the pseudo-Hermitian approach the energies are preserved when transforming from the non-Hermitian to the Hermitian system by means of a Dyson map. Legitimised in this way, we focused in sections 4-7 on the energies of several variants of the BPS Skyrme model. Despite being complex, the topology of our field solutions at infinity determine unambiguously the energy of such solutions by their asymptotic behaviour. In these models one needs to be cautious of over-interpreting other properties of the solutions within the context of non-Hermitian theories that will not be preserved when transformed by means of Dyson maps to solutions of the corresponding Hermitian system.

CRediT authorship contribution statement

All authors contributed in equal terms.

Declaration of competing interest

The authors declare that they have no known competing financial interests or personal relationships that could have appeared to influence the work reported in this paper.

Acknowledgements

References

[1] T.H.R. Skyrme, A unified field theory of mesons and baryons, Nucl. Phys. 31 (1962) 556–569.
[2] E. Witten, Global aspects of current algebra, Nucl. Phys. B 223 (1983) 422–432.
[3] E. Witten, Current algebra, baryons, and quark confinement, Nucl. Phys. B 223 (1983) 433–444.
[4] G.S. Adkins, C.R. Nappi, The Skyrme model with pion masses, Nucl. Phys. B 233 (1) (1984) 109–115.
[5] R.A. Battye, P.M. Sutcliffe, Skyrmions with massive pions, Phys. Rev. C 73 (5) (2006) 055205.
[6] D. Harland, Topological energy bounds for the Skyrme and Faddeev models with massive pions, Phys. Lett. B 728 (2014) 518–523.
[7] U.-G. Meissner, I. Zahed, Skyrmions in the presence of vector mesons, Phys. Rev. Lett. 56 (10) (1986) 1035.
[8] M. Bando, T. Kugo, S. Uehara, K. Yamawaki, T. Yanagida, Is the ρ meson a dynamical gauge boson of hidden local symmetry?, Phys. Rev. Lett. 54 (12) (1985) 1215.
[9] D. Finkelstein, J. Rubinstein, Connection between spin, statistics, and kinks, J. Math. Phys. 9 (11) (1968) 1762–1779.
[10] L. Faddeev, Some comments on the many-dimensional solitons, Lett. Math. Phys. 1 (4) (1976) 289–293.
[11] M.F. Atiyah, N.S. Manton, Skyrmions from instantons, Phys. Lett. B 222 (3–4) (1989) 438–442.
[12] P. Sutcliffe, Skyrmions, instantons and holography, J. High Energy Phys. 2010 (8) (2010) 19.
[13] G.S. Adkins, C.R. Nappi, E. Witten, Static properties of nucleons in the Skyrme model, Nucl. Phys. B 228 (3) (1983) 552–566.
[14] R.A. Battye, P.M. Sutcliffe, Solitonic fullerene structures in light atomic nuclei, Phys. Rev. Lett. 86 (18) (2001) 3989.
[15] R.A. Battye, P.M. Sutcliffe, Skyrmions, fullerenes and rational maps, Rev. Math. Phys. 14 (01) (2002) 29–85.
[16] S. Krusch, Homotopy of rational maps and the quantization of Skyrmions, Ann. Phys. 304 (2) (2003) 103–127.
[17] D.T.J. Feist, P.H.C. Lau, N.S. Manton, Skyrmions up to baryon number 108, Phys. Rev. D 87 (8) (2013) 085034.

[18] M. Gillard, D. Harland, M. Speight, Skyrmions with low binding energies, Nucl. Phys. B 895 (2015) 272–287.

[19] N. Manton, P. Sutcliffe, Topological Solitons, CUP, Cambridge, 2004.

[20] E.B. Bogomolny, The stability of classical solutions, Sov. J. Nucl. Phys. 24 (4) (1976) (Engl. Transl.) (United States).

[21] M.K. Prasad, C.M. Sommerfield, Exact classical solution for the 't Hooft monopole and the Julia-Zee dyon, Phys. Rev. Lett. 35 (12) (1975) 760.

[22] C. Adam, J. Sanchez-Guillen, A. Wereszczyński, A Skyrme-type proposal for baryonic matter, Phys. Lett. B 691 (2) (2010) 105–110.

[23] C. Adam, C. Naya, J. Sanchez-Guillen, A. Wereszczynski, Bogomolnyi-Prasad-Sommerfield Skyrme model and nuclear binding energies, Phys. Rev. Lett. 111 (23) (2013) 232501.

[24] E. Bonenfant, L. Marleau, Nuclei as near BPS Skyrmions, Phys. Rev. D 82 (5) (2010) 054023.

[25] E. Bonenfant, L. Harbour, L. Marleau, Near-BPS Skyrmions: nonshell configurations and Coulomb effects, Phys. Rev. D 85 (11) (2012) 114045.

[26] C. Adam, C. Naya, J. Sanchez-Guillen, R. Vazquez, A. Wereszczyński, The Skyrme model in the BPS limit, in: The Multifaceted Skyrmion, World Scientific, 2017, pp. 193–232.

[27] A. Fring, T. Taira, Complex BPS solitons with real energies from duality, J. Phys. A, Math. Theor. 53 (45) (2020) 455701.

[28] E. Wigner, Normal form of antiunitary operators, J. Math. Phys. 1 (1960) 409–413.

[29] C.J. Houghton, N.S. Manton, P.M. Sutcliffe, Rational maps, monopoles and Skyrmions, Nucl. Phys. B 510 (3) (1998) 507–537.

[30] S.B. Gudnason, Exploring the generalized loosely bound Skyrme model, Phys. Rev. D 98 (9) (2018) 096018.

[31] C. Adam, K. Oles, A. Wereszczynski, The dielectric Skyrme model, Phys. Lett. B 807 (2020) 135560.

[32] C.M. Bender, P.E. Dorey, C. Dunning, A. Fring, D.W. Hook, H.F. Jones, S. Kuzhel, G. Levai, R. Tateo, P.T. Symmetry, in: Quantum and Classical Physics, World Scientific, Singapore, 2019.

[33] A. Mostafazadeh, Pseudo-Hermitian representation of quantum mechanics, Int. J. Geom. Methods Mod. Phys. 7 (2010) 1191–1306.

[34] C.M. Bender, H.F. Jones, R.J. Rivers, Dual $\mathcal{PT}$-symmetric quantum field theories, Phys. Lett. B 625 (2005) 333–340.

[35] P. Rosenau, J.M. Hyman, Compactons: solitons with finite wavelength, Phys. Rev. Lett. 70 (5) (1993) 564–567.

[36] C. Adam, L.A. Ferreira, E. Da Hora, A. Wereszczynski, W.J. Zakrzewski, Some aspects of self-duality and generalised BPS theories, J. High Energy Phys. 2013 (8) (2013) 62.

[37] S.B. Gudnason, M. Nitta, S. Sasaki, A supersymmetric Skyrme model, J. High Energy Phys. 2016 (2) (2016) 74.

[38] S.B. Gudnason, M. Nitta, S. Sasaki, Topological solitons in the supersymmetric Skyrme model, J. High Energy Phys. 2017 (1) (2017) 14.

[39] A. Fring, T. Taira, Goldstone bosons in different PT-regimes of non-Hermitian scalar quantum field theories, Nucl. Phys. B 950 (2020) 114834.

[40] C.M. Bender, S. Boettcher, Real spectra in non-Hermitian Hamiltonians having PT symmetry, Phys. Rev. Lett. 80 (1998) 5243–5246.

[41] C. Adam, J. Sanchez-Guillen, A. Wereszczynski, BPS submodels of the Skyrme model, Phys. Lett. B 769 (2017) 362–367.